OM-X®, Fermented Vegetables Extract Suppresses Antigen-Stimulated Degranulation in Rat Basophilic Leukemia RBL-2H3 Cells and Passive Cutaneous Anaphylaxis Reaction in Mice

Tomohiro Itoh*[a], Yasuyoshi Miyake[b], Takuya Kasashima[a], Yoshie Shimomiya[b], Yuki Nakamura[b], Masashi Ando[a], Yasuyuki Tsukamasa[a] and Muneaki Takahata[b]

[a]*Laboratory of Aquatic Food Science, Department of Fisheries, Faculty of Agriculture, Kinki University, 3327-204 Nakamachi, Nara 631-8505, Japan*

[b]*BIOBANK Co., Ltd., 388-1 Kita-ku, Okayama 700-0952, Japan*

titoh@nara.kindai.ac.jp

OM-X® is a hand-made and naturally manufactured probiotic supplement. This fermented food product is made from vegetables, fruits, seaweeds and mushrooms, using 12 strains of lactic acid bacteria and bifidobacteria. OM-X® is also known to have beneficial health properties, and some of its components show effects on antigen (Ag)-stimulated degranulation activity, indicating that OM-X® may be useful in the treatment of allergy responses and symptoms. In this study, we evaluated the inhibitory effects of OM-X® on Ag-stimulated degranulation in rat basophilic leukemia RBL-2H3 cells, clarified the underlying mechanisms, and determined the active compounds in OM-X® for suppression of degranulation. Treatment with OM-X® gradually suppressed Ag-stimulated degranulation throughout the maturation period. OM-X® also gradually produced melanoidins by lactic acid bacterial fermentation during the maturation process. There was a high correlation between the suppression levels of Ag-stimulated degranulation and the browning of OM-X®. Furthermore, the inhibition of Ag-stimulated degranulation by OM-X® was found to be partially due to the direct inactivation of NADPH oxidase. To elucidate the *in vivo* effects of OM-X®, type I allergy model mice were orally administered with OM-X®, and the passive cutaneous anaphylaxis (PCA) reaction was measured. OM-X® intake remarkably suppressed the PCA reaction. Taken together, our findings suggest that OM-X® could be a beneficial food to ameliorate allergic reactions.

Keywords: OM-X®, Degranulation, Type I allergy, RBL-2H3 cells, Melanoidin.

Type I allergy or immediate-type hypersensitivity is implicated in various allergic symptoms including rhinitis, conjunctivitis, bronchial asthma, and urticarial. Mast cells are the key effector cells that cause these allergic symptoms. High-affinity immunoglobulin E (IgE) receptor (FcεRI) is expressed on the surface of mast cells and basophils, and IgE binds to the FcεRIα chain. Cross-linking of IgE-mediated by the binding of multivalent antigen on the surfaces of mast cells induces the release of intragranular mediators such as histamine, arachidonic acid metabolites, proteases, serotonin, and heparin [1-4]. These mediators then trigger immediate allergic responses.

OM-X® is a probiotic supplement that was manufactured by Dr Iichiroh Ohhira using a unique fermentation method. It is strictly hand-made and is comprised of all natural components. OM-X® is a naturally fermented mixture of vegetables, fruits, seaweeds, and mushrooms, using 12 strains of lactic acid bacteria (LAB) and bifidobacteria. After 5 years of fermentation at room temperature, the fermented mixture contains probiotics, prebiotics such as oligosaccharides and dietary fiber, and trace amounts of vitamins, minerals, short-chain fatty acids, and amino acids (Figure 1). In human clinical studies, OM-X® has shown beneficial effects on bone health [5], oral ulcerations [6], and colitis [7].

Recent studies demonstrated that carotenoids and flavonoids, which are present in the ingredients used in the manufacturing of OM-X®, show effects on antigen (Ag)-stimulated degranulation [8,9]. Natural materials that are fermented by LAB such as grape marc, have also been shown to suppress the type I allergic response, and thus, it seems, the allergy symptoms. Moreover, OM-X® gradually produces melanoidins by LAB fermentation during the maturation
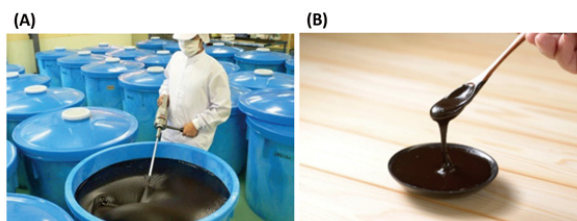

Figure 1: The making process and appearance of OM-X®. (A) The maturation process of OM-X®. (B) The image of 5 years-matured OM-X®.

process. However, scarce information is available on the relationship between melanoidins and allergy. The aim of this study was to evaluate the inhibitory effects of OM-X® on Ag-stimulated degranulation in rat basophilic leukemia RBL-2H3 cells, clarify the underlying mechanisms, and determine the active compounds in OM-X® for the suppression of degranulation. Furthermore, we evaluated the ability of oral administration of OM-X® to inhibit type I allergy symptoms in model mice.

In the present study, we evaluated the anti-degranulation activity of OM-X® and the underlying inhibitory mechanisms on Ag-challenged degranulation. OM-X® resulted in gradual inhibition of Ag-stimulated degranulation in RBL-2H3 cells, and the inhibitory effect increased in a time- and dose-dependent manner (Figure 2). Interestingly, there was a high correlation between the inhibitory activities of OM-X® on Ag-stimulated degranulation in RBL-2H3 cells and the browning of OM-X® (R = 0.9802, Figure 2A and Figure 3). OM-X® is made from natural ingredients (44%, w/w), sugar (55.4%, w/w), and 12 strains of LAB and bifidobacteria (0.6%). During the maturation, amino acids derived from the

mixture of natural ingredients react with sugar owing to the heat produced during fermentation (Maillard reaction), generating the brown melanoidins. Thus, it was considered that the carotenoids [10] and flavonoids [11,12] contained in the ingredients used for making OM-X® had no effect on the Ag-stimulated degranulation, as these compounds would likely be broken down by fermentation. Since melanoidins are well known to function as antioxidant/radical-scavengers [13-15], we measured the DPPH radical scavenging activity of OM-X®. The antioxidant activities of 5-year-matured OM-X® were dramatically increased 5.3-fold compared with those of 1-year-matured OM-X®. There was also a high correlation between the browning of OM-X ® and its antioxidant activity (R = 0.9787), indicating that these scavenging activities were likely involved in the generation of melanoidins during the maturation process. The half-maximal concentration (ED_{50}) for the antioxidant activities of 5-year- matured OM-X® was approximately 200 μg/mL (Figure 4A), which was 20-fold lower than that of L-ascorbic acid (positive control, Figure 4B). Collectively, these results suggest that the melanoidins generated during fermentation contribute to inhibition of Ag-stimulated degranulation in RBL-2H3 cells.
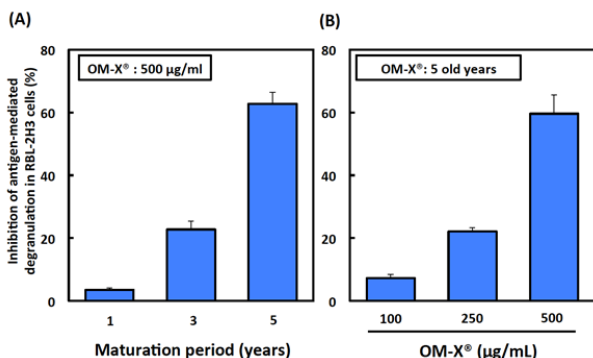

Figure 2: The inhibitory effects of OM-X® on Ag-stimulated β-hexosaminisase release. (A) Maturation time dependency (B) Dose dependency. Values are given as mean±S.E. (n=12).

To gain further insight into the mechanisms underlying the inhibitory effects of OM-X® on Ag-stimulated degranulation, we first measured the changes of intracellular ROS production and the levels of Ca^{2+} mobilization in Ag-stimulated RBL-2H3 cells treated with or without OM-X®. As shown in Figure 5, 250 μg/mL of OM-X suppressed ROS production to the same extent as diphenyleneiodonium (DPI). OM-X® also suppressed the levels of Ca^{2+} mobilization to a similar level observed in untreated cells (Figure 6). Furthermore, OM-X® suppressed the translocation of Rac, a cytosolic subunit of NADPH oxidase, to the plasma membrane (Figure 7). These results demonstrate that the general mechanism of degranulation inhibition involves direct inactivation of NADPH oxidase. Upon Ag-stimulated degranulation, the level of intracellular ROS is elevated by NADPH oxidase activation. NADPH oxidase is an enzyme complex composed of membrane-bound subunits ($gp91^{phox}$ and $p22^{phox}$), cytosolic subunits ($p40^{phox}$, $p47^{phox}$, and $p67^{phox}$), and a monomeric GTP-binding protein of the Rho family Rac [16,17]. To activate phagocytic NADPH oxidase, the cytosolic subunits are translocated to the membrane, thus initiating production of superoxide [18]. The superoxide produced following Ag stimulation is then readily converted to hydrogen peroxide, which in turn regulates the Ca^{2+} channel on the cell surface, thus controlling Ca^{2+} influx from the extracellular medium [19]. After Ag stimulation, signal transduction for degranulation and cytokine production in mast cells is immediately activated following aggregation of FcεRI [20]. Translocation of cytosolic
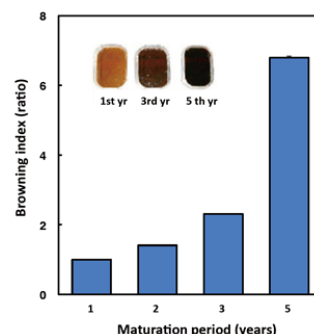

Figure 3: The changes in browning index in OM-X® during maturation. The values are given as mean±S.E. (n=10).
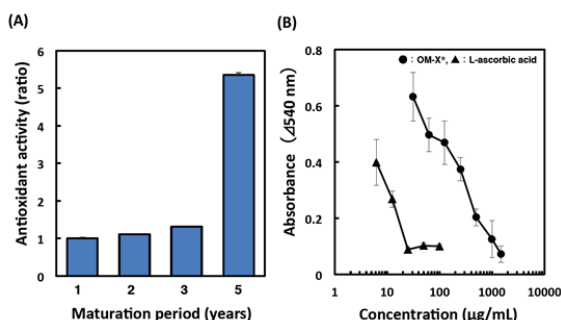

Figure 4: Antioxidative activity of OM-X®. (A) The changes in antioxidative activities in OM-X® during maturation. (B) The antioxidative activity of 5 years-matured OM-X®. L-Ascorbic acid was used as an anti-oxidative positive control. Values are given as mean±S.E. (n=16).

subunits of NADPH oxidase to membrane-bound subunits proceeds through the phosphorylation of Syk. Thus, we further examined the early intracellular signaling transduction pathways involved in OM-X® on suppressing the responses to Ag stimulation. The data presented in Figure 8 show that OM-X® treatment had no effect on the Lyn/Syk/PLCγ pathway, PI3K/Akt, and MAP kinases in Ag-challenged RBL-2H3 cells. Thus, the production of intracellular ROS was due to the direct suppression of the translocation of cytosolic subunits of NADPH oxidase and the scavenging of ROS by OM-X®'s own antioxidative activity (Figure 9).
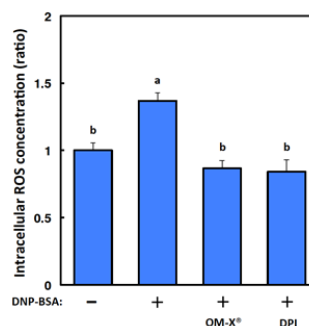

Figure 5: Effects of OM-X® on intracellular ROS production in Ag-stimulated RBL-2H3 cells. IgE-sensitized RBL-2H3 cells were treated with 10 μM CM-H₂DCF-DA and incubated with or without OM-X® or 200 nM diphenyleneiodonium (DPI) for 30 min. Cells were then stimulated with or without DNP-BSA. Values are given as mean±S.E. (n=16). Means not sharing a common letter in a column were significantly different, $p < 0.05$, Tukey-Kramer multiple group comparison test.

To examine the effect of OM-X® on the type I allergy response, we evaluated the PCA reaction in type I allergy model mice. Oral administrations of OM-X® (low-dose group: 2.5 g·60 kg body weight^{-1}·day^{-1}, high-dose group; 5.0 g·60 kg body weight^{-1}·day^{-1}) decreased the amount of extravasated dye in a dose-dependent
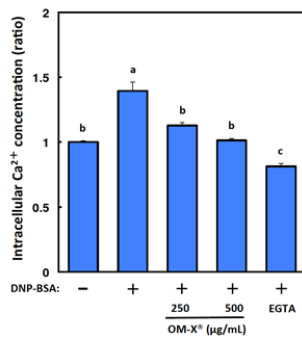
Figure 6: Effects of OM-X® on the elevation of intracellular Ca^{2+} in Ag-stimulated RBL-2H3 cells. IgE-sensitized RBL-2H3 cells were treated with Fluo-3AM and incubated with or without OM-X® or 1 mM ethylene glycol tetra acetic acid (EGTA, Ca^{2+} chelator) for 30 min. Cells were then stimulated with or without DNP-BSA, after which intracellular Ca^{2+} levels were measured by a fluorometric imaging plate reader. Values are given as mean$\pm$S.E. (n=10). Means not sharing a common letter in a column were significantly different, $p < 0.05$, Tukey-Kramer multiple group comparison test.

Figure 7: OM-X® suppresses translocation of Rac to the membrane. A representative blot from 3 independent experiments is shown.

Figure 8: Effects of OM-X® on Ag-stimulated activation of intracellular signaling pathways in RBL-2H3 cells. IgE-sensitized RBL-2H3 cells were treated with or without 250 μg/mL OM-X® for 30 min. The cells were then stimulated with or without DNP-BSA. Cell lysates were analyzed by Western blot for the indicated proteins. A representative blot from 3 independent experiments is shown.
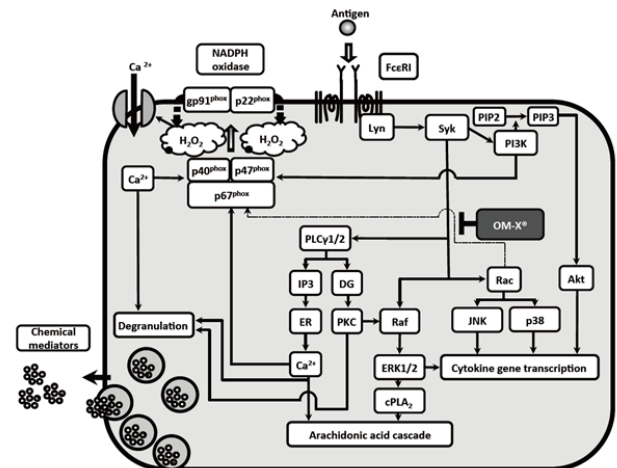

Figure 9: Scheme showing the inhibitory effects of OM-X® on Ag-stimulated degranulation in mast cells. OM-X® attenuates intracellular ROS production through the inhibition of Rac translocation.
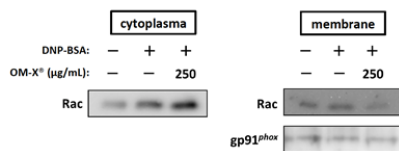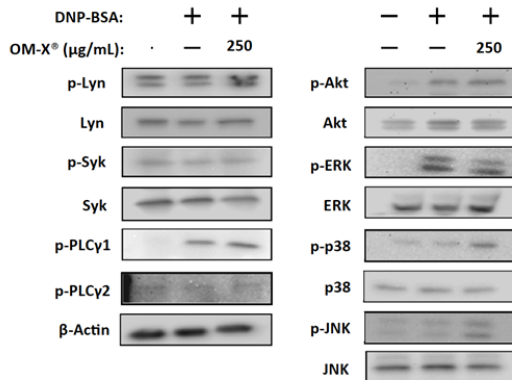

Figure 10: Inhibitory effects of oral intake of OM-X® on PCA reaction in ICR mice. ICR mice fed with or without OM-X® for 4 weeks were given injection of anti-DNP IgE. Twenty-four hours later, PBS containing DNP–BSA and Evans blue dye were intravenously injected. One hour later, mice were sacrificed and their dorsal skin was photographed. Photographs shown represent three independent experiments, each containing six mice per group. Sham represents mice injected with IgE and Evans blue dye, but without DNP–BSA (left panel). After taking photographs, the amounts of Evans blue dye extracted from skin were determined. The inhibition of PCA reaction was expressed as a percentage of Evans blue content in control water-fed mice (right panel). Values are given as mean$\pm$S.E. (n=10). Means not sharing a common letter in a column were significantly different, $p < 0.05$, Tukey-Kramer multiple group comparison test.

manner (Figure 10). In particular, the PCA reaction was suppressed to the same extent in the high-dose group as in the negative control group, which was treated with anti-DNP-IgE without Ag stimulation. Therefore, OM-X® intake likely contributes to suppression of allergic symptoms, and would be a beneficial natural material for the treatment of type I allergy.

Taken together, our findings suggest that the inhibitory effect of OM-X® on Ag-stimulated degranulation was due, at least in part, to the suppression of intracellular Ca^{2+} mobilization through inhibition of the translocation of cytosolic subunits of NADPH oxidase to membrane-bound subunits and direct scavenging of ROS that are produced by NADPH oxidase.
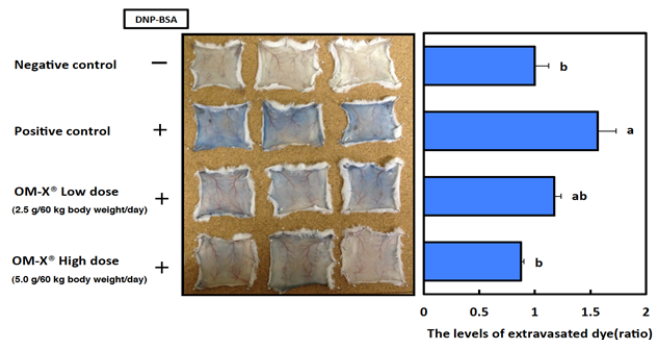
Experimental

Reagents and materials: Mouse anti-dinitrophenol (DNP) monoclonal IgE was purchased from Yamasa (Tokyo, Japan). The $25 \times$ Complete®, a mixture of proteinase inhibitors and the phosphatase inhibitor PhoSTOP® were from Roche (Penzberg, Germany). The antibodies to Akt, phospho-Akt, p44/42 MAPkinase (ERK), phospho- p44/42 MAPkinase (Thr202/tyr204) (p-ERK), SAPK/JNK (JNK), phospho- SAPK/JNK (Thr183/Tyr185) (p-JNK), p38 MAP kinase (p38), phospho-p38 MAP kinase (Thr180/Tyr182) (p-p38), Lyn, phospho-Lyn, phospho-PLCγ1, phospho-PLCγ2, Syk, and Rac were from Cell Signaling Technology (MA, USA). The antibody to gp91^{phox} was from Santa Cruz Biotechnology (CA, USA). The antibody to was phospho-Syk (p-Syk) from Abcam (MA, USA).

Cell culture: RBL-2H3 cells were obtained from the Health Science Research Resource Bank (Tokyo, Japan). Cells were grown in Eagle's minimum essential medium (Life Technologies; Carlsbad, CA, USA) containing 10% heat-inactivated fetal bovine serum, 100 U/mL of penicillin, and 100 mg/mL of streptomycin in a humidified atmosphere of 5% CO_2 at 37°C.

OM-X® preparation: The OM-X® sample was provided by BIOBANK Co., Ltd. (Okayama, Japan). All plant ingredients used in OM-X® are nutritionally rich and safe for human consumption. The general procedure involves loading each ingredient into the manufacturing vats one by one at the different stages of fermentation. When each ingredient is added, it is fermented by LAB to produce various organic acids and amino acids. In addition, the solid ingredients are broken down to facilitate absorption of their components through fermentation. Thus, various ingredients that are beneficial to human health are fermented and matured for 5 years. In the OM-X® used in the current study, 12 strains of LAB were added to ferment and mature the plant ingredients. One of the strains has very high proteolytic capability, which was isolated and identified from tempeh. The specific ingredients used for OM-X® production and the composition of organic acids and carbohydrates in OM-X® are shown in Tables 1 and 2. OM-X® was determined to be safe for human consumption with no adverse health effects, according to a single-dose oral toxicity test conducted by Mitsubishi Chemical Safety Institute Ltd. (Tokyo, Japan).

Table 1: Composition of food materials for making of OM-X.

Fruits:
Prune, Fig, Chinese bayberry, Chinese matrimony, Blueberry, Yuzu (lemon)

Vegetables:
Japanese mugwort, Komatsuna

Mushrooms:
Shiitake mushroom, Maitake (dancing mushroom), Agaricus mushroom

Seaweeds:
Wakame (brown seaweed), Hijiki seaweeed, Konbu (Kelp)

Sugar

Lactic acid bacteria:
Bifidobacterium breve ss. breve, Bifidobacterium infantis ss. infantis, Bifidobacterium longum, Enterococcus faecalis, Lactobacillus acidophilus, Lactobacillus brevis, Lactobacillus bulgaricus, Lactobacillus casei ss. casei, Lactobacillus fermentum, Lactobacillus helveticus ss. jugurti, Lactobacillus plantarum, Streptococcus thermophilus

Table 2: Composition of organic acids and carbohydrates in OM-X.

Citric acid	Glucose
Lactic acd	Fructose
Malic acid	Galactose
Formic acid	Mannose
Acetic acid	Isomaltose
Succinic acid	Panose

Degranulation assay

β-Hexosaminidase release assay: We used β-hexosaminidase as a marker of degranulation. RBL-2H3 cells (2×10^4 cells/well) were seeded onto 24-well plates and cultured for 12 h. Cells were then treated with anti- DNP-IgE (0.45 μg/mL) and incubated for 24 h. After washing twice with Siraganian buffer A (119 mM NaCl, 5 mM KCl, 0.4 mM MgCl$_2$, 25 mM PIPES, and 40 mM NaOH, pH 7.2), 160 μL of Siraganian buffer B {5.6 mM glucose, 1 mM CaCl$_2$, and 0.1% bovine serum albumin (BSA)} was added to each well. After incubating at 37°C for 10 min, cells were treated with the OM-X® at 37°C for a further 30 min. DNP-labeled BSA (DNP-BSA; 20 μL) was then added to the culture medium to a final concentration of 10 μg/mL. After 10 min, cells were placed on ice for 10 min to terminate the reaction. The supernatants were then harvested by centrifugation at $300 \times g$ at 4°C for 10 min. The supernatants (50 mL) were transferred into 96-well microplates and allowed to react with 50 μL of 0.1 M citrate buffer (pH 4.5) that contained 1 mM *p*-nitrophenyl-*N*-acetyl-β-D-glucosaminide (CB-PNAG) at 37°C. The reaction was terminated after 1 h by adding stop buffer (0.1 M Na$_2$CO$_3$/NaHCO$_3$, pH 10.0). Absorbance was measured at 405 nm using a colorimetric microplate reader (Corona Grating Microplate Reader SH-9000, Corona Electric Co. Ltd.; Hitachinaka, Ibaraki, Japan).

β-Hexosaminidase inhibitory activity: Samples (5 μL) and conditioned medium prepared from Ag-stimulated RBL-2H3 cells (45 μL) were placed in the wells of 96-well microplates, and reacted with 50 μL of 0.1 M CB-PNAG at 37°C for 1 h. After terminating the reaction, the absorbance at 405 nm was measured. The inhibition of degranulation was calculated as follows:

Inhibition of degranulation (%) = [1− ($A_{405 \text{ nm of sample}}$ − $A_{405 \text{ nm negative control}}$) / ($A_{405 \text{ nm positive control}}$ − $A_{405 \text{ nm negative control}}$)] × 100 - β-hexosaminidase inhibitory activity (%)

β-Hexosaminidase inhibitory activity (%) = [1− ($A'_{405nm \text{ of sample}}$ − $A'_{405nm \text{ negative control}}$) / ($A'_{405nm \text{ positive control}}$ − $A'_{405nm \text{ negative control}}$)] × 100

Measurement of intracellular Ca²⁺ concentrations: Intracellular Ca^{2+} levels were determined with a Calcium Kit-Fluo 3™ (Dojindo Laboratories; Kumamoto, Japan). RBL-2H3 cells (5×10^4 cells/well) were seeded onto 96-well microplates and incubated for 1 h. The cells were then treated with anti-DNP IgE (0.45 μg/mL) and incubated for 24 h. After washing twice with phosphate-buffered saline (PBS), 100 μL of loading buffer containing Fluo-3AM (Calcium Kit-Fluo 3™) was added to the culture medium. One hour later, the cells were washed with PBS and incubated in 90 μL of loading buffer containing OM-X®. After incubation for 30 min, cells were stimulated by DNP-BSA (10 μg/mL) and the fluorescence was measured using a fluorometric imaging plate reader (excitation: 490 nm, emission: 530 nm).

Measurement of intracellular reactive oxygen species (ROS) levels: Intracellular ROS levels were measured by using the general marker of oxidative stress CM-H$_2$DCF-DA. IgE-sensitized RBL-2H3 cells (5×10^4 cells/well) were incubated with 10 μM CM-H$_2$DCF-DA for 30 min at 37°C. After washing twice with Siraganian buffer A, cells were incubated with Siraganian buffer B including OM-X® for 30 min. Then, the cells were stimulated with DNP-BSA (10 μg/mL), and the fluorescence was measured using the fluorometric imaging plate reader (excitation: 490 nm, emission: 530 nm).

Measurement of DPPH radical-scavenging activity: To measure *in vitro* anti-oxidant activity, the DPPH radical-scavenging assay was carried out as described previously. Briefly, 180 μL of 0.2 mM DPPH radical solution and 20 μL of OM-X® were rapidly mixed and the decrease in absorbance at 517 nm was monitored. DPPH free radical-scavenging activity (%) was calculated using the following formula:

[($A_{517nm \text{ of control}}$ − $A_{517nm \text{ of sample}}$) / $A_{517nm \text{ of control}}$] × 100

Vitamin C (L-ascorbic acid, Wako Pure Chemical Co. Ltd.; Osaka, Japan), a potent anti-oxidant, was used as a positive control.

Immunoblot analysis: Cell lysates were prepared as described previously. The cytosolic and membrane fractions were separated

using the ProteoExtract subcellular proteome extraction kit (Merck KGaA; Darmstadt, Germany). Protein samples were subjected to sodium dodecyl sulfate–polyacrylamide gel electrophoresis (SDS-PAGE), and then transferred onto polyvinylidene fluoride membranes. After blocking for 1 h in 5% non-fat milk, the membrane was incubated with a primary antibody at 4°C overnight, followed by incubation with a horseradish peroxidase-conjugated secondary antibody at room temperature for 1 h. Immunoreactive proteins were detected with an enhanced ECL kit and a Davinch-Chemilumino-image analyzer (Wako).

Animals and diets: Four-week-old ICR male mice (Japan SLC, Ltd.; Hamamatsu, Japan) were housed in an air-conditioned room (22±2°C) with a 12-h light and dark cycle (lighting from 0700 to 1900). All mice were fed commercial CE-2 pellets (Clea Japan Inc.; Tokyo, Japan) and water *ad libitum* for 1 week to acclimatize them to their surroundings. After 1 week, each mouse was treated with 100 μL of either PBS or OM-X® (2.5 or 5.0 g/60 Kg body weight/day) by oral administration for 4 weeks. This study was approved by the Kinki University Animal Use Committee, and animals were maintained according to the guidelines of the Kinki University for the care of laboratory animals.

Measurement of the mouse passive cutaneous anaphylaxis (PCA) reaction: The IgE-induced PCA reaction was measured according to a previously published method [21], with the following slight modification. The back hair of the ICR mice was shaved, and 10 mg of anti-DNP-IgE was injected into 2 dorsal skin sites per mouse. The sites were outlined with a water-insoluble marker. Twenty four hours later, each mouse received an injection of 200 μL of DNP-BSA of 1% Evans blue (Sigma) in PBS, containing 200 μg of DNP-BSA. Treated mice were sacrificed 1 h later, and their dorsal skin was removed. Skin pieces (1 cm) were dissolved with 1 N KOH at 37°C for 24 h, and the extravasated Evans blue dye was extracted with a mixture of acetone and 0.2 M phosphoric acid (13:5) from the treated skin solution. The amount of dye was determined colorimetrically at 620 nm.

Statistical analysis: All data were analyzed using the Mac statistical analysis software package for Macintosh, version 2.0 (Esumi Co.; Tokyo Japan). All data are expressed as means ± standard error (S.E.). Statistical analysis was performed using the Tukey-Kramer test for comparisons among many groups or the Student's *t*-test for comparisons between 2 groups, at a significance level of $p < 0.01$.

References

[1] Beaven MA, Metzger H. (**1993**) Signal transduction by Fc receptors: FcεRI case. *Immunology Today*, **14**, 222-226.
[2] Turner H, Kinet JP. (**1999**) Signalling through the high-affinity IgE receptor FcεRI. *Nature*, **402**, B24-30.
[3] Mekori YA, Metcalfe DD. (**2000**) Mast cells in innate immunity. *Immunological Reviews*, **173**, 131-140.
[4] Kalesnikoff J, Galli SJ. (**2008**) New developments in mast cell biology. *Nature Immunology*, **9**, 1215-1223.
[5] Kawakami M, Ohhira I, Araki N, Inokihara K, Iwasaki H, Matsubara T. (**2003**) The influence of lactic acid bacteria (OM-X) on bone structure. *The Journal of Applied Nutrition*, **53**, 2-8.
[6] Hashim, BY, Rahman RA, Philip K. (**1999**) Lactic acid bacteria is beneficial for oral aphthous ulcerations. *Annals of Dentistry*, **1**, 44-47.
[7] Takahata M, Fremont M, Desreumaux P, Rousseaux C, Dubuquoy C, Shimomiya Y, Nakamura Y, Miyake Y. (**2014**) Evaluation of therapeutic properties of fermented vegetable extract (OM-X®) in the model of colitis induced by *Citrobacter rodentium* in mice. *Journal of Functional Foods*, **10**, 117-127.
[8] Itoh T, Ninomiya M, Yasuda M, Koshikawa K, Deyashiki Y, Nozawa Y, Akao Y, Koketsu M. (**2009**) Inhibitory effects of flavonoids isolated from *Fragaria ananassa* Duch on IgE-mediated degranulation in rat basophilic leukemia RBL-2H3. *Bioorganic & Medicinal Chemistry*, **17**, 5374-5379.
[9] Manabe Y, Hirata T, Sugawara T. (**2014**) Suppressive effects of carotenoids on the antigen-induced degranulation in RBL-2H3 rat basophilic leukemia cells. *Journal of Oleo Science*, **63**, 291-294.
[10] Sugawara T, Ganesan P, Li Z, Manabe Y, Hirata T. (**2014**) Siphonaxanthin, a green algal carotenoid, as a novel functional compound. *Marine Drugs*, **12**, 3660-3668.
[11] Tanaka T, Takahashi R. (**2013**) Flavonoids and asthma. *Nutrients*, **5**, 2128-2143.
[12] Tanaka T. (**2014**) Flavonoids for allergic diseases: present evidence and future perspective. *Current Pharmaceutical Design*, **20**, 879-885.
[13] Chuyen NV, Ijichi K, Umetsu H, Moteki K. (**1998**) Antioxidative properties of products from amino acids or peptides in the reaction with glucose. *Advances in Experimental Medicine and Biology*, **434**, 201-212.
[14] Lindenmeier M, Faist V, Hofmann T. (**2002**) Structural and functional characterization of poly-lysine, a novel protein modification in bread crust melanoidins showing *in vitro* antioxidative and phase I/II enzyme modulating activity. *Journal of Agricultural Food Chemistry*, **50**, 6997-7006.
[15] Bekedam EK, Schols HA, Cammerer B, Kroh LW, van Boekel MA, Smit G. (**2008**). Electron spin resonance (ESR) studies on the formation of roasting-induced antioxidative structures in coffee brews at different degrees of roast. *Journal of Agricultural Food Chemistry*, **56**, 4597-4604.
[16] Sarfstein R, Gorzalczany Y, Mizrahi A, Berdichevsky Y, Molshanski-Mor S, Weinbaum C, Hirshberg M, Dagher MC, Pick E. (**2004**) Dual role of Rac in the assembly of NADPH oxidase, tethering to the membrane and activation of p67phox: a study based on mutagenesis of p67phox-Rac1 chimeras. *The Journal of Biological Chemistry*, **279**, 16007-16016.
[17] Cross AR, Segal AW. (**2004**) The NADPH oxidase of professional phagocytes-prototype of the NOX electron transport chain systems. *Biochimica et Biophysica Acta*, **1657**, 1-22.
[18] Bedard K, Krause KH. (**2007**) The Nox family of ROS-generating NADPH oxidases: physiology and pathophysiology. *Physiological Reviews*, **87**, 245-313.
[19] Yoshimaru T, Suzuki Y, Matsui T, Yamashita K, Ochiai T, Yamaki M, Shimizu K. (**2002**) Blockade of superoxide generation prevents high-affinity immunoglobulin E receptor-mediated release of allergic mediators by rat mast cell line and human basophils. *Clinical & Experimental Allergy*, **32**, 612-618.
[20] Sibilano R, Frossi B, Pucillo CE. (**2014**) Mast cell activation: a complex interplay of positive and negative signaling pathways. *European Journal of Immunology*, **44**, 2558-2566.
[21] Choo, MK, Park EK, Han MJ, Kim DH. (**2003**) Antiallergic activity of ginseng and its ginsenosides. *Planta Medica*, **69**, 518-522.